Hindawi
Nanomaterials and Nanotechnology
Volume 2023, Article ID 7790674, 13 pages
https://doi.org/10.1155/2023/7790674

Research Article

Nanomaterials in Nanophotonics Structure for Performing All-Optical 2 × 1 Multiplexer Based on Elliptical IMI-Plasmonic Waveguides

Sajjad Mohanad Mustafa,[1] **Gholamreza Karimi**,[1] **Mazdak Rad Malek Shahi**,[1] **and Saif Hasan Abdulnabi**[2,3,4]

[1]*Electrical Engineering Department, Faculty of Electrical and Computer Engineering, Razi University, 6714967346, Kermanshah, Iran*
[2]*Department of Electronic and Communications Engineering, Faculty of Engineering, University of Kufa, Kufa Street, Najaf 54001, Iraq*
[3]*Department of Electrical Engineering, College of Engineering, University of Baghdad, Al-Jadriya, Baghdad 10001, Iraq*
[4]*Department of Computer Techniques Engineering, Information Technology College, Imam Ja'afar Al-Sadiq University, Maysan Street, Najaf 54001, Iraq*

Correspondence should be addressed to Gholamreza Karimi; ghkarimi@razi.ac.ir

Received 10 May 2023; Revised 29 July 2023; Accepted 17 October 2023; Published 8 November 2023

Academic Editor: Andres Cantarero

In this study, an all-optical multiplexer (Mux) based on elliptical insulator-metal-insulator (IMI) plasmonic waveguides is designed. The area of the proposed structure is very small (400 nm × 400 nm) which operates at a wavelength of 1,550 nm. The developed device utilizes constructive and destructive interferences between the input signals and the selector signal. This structure is less complex and has lower loss compared to the previous works. Transmission (T), contrast ratio (CR), modulation depth (MD), insertion loss (IL), and contrast loss (CL) are the five parameters that describe the performance of the plasmonic Mux. The transmission threshold between logic 0 and logic 1 is 0.5. Moreover, the maximum transmission efficiency of the device is 163%. Moreover, based on the MD value of 95.09%, the dimensions of the proposed structure are excellent and optimal. The proposed plasmonic Mux structure contributes substantially to developing an all-optical arithmetic logic unit (ALU) and all-optical signal processing nanocircuits. The finite element method (FEM) simulates the proposed plasmonic multiplexer with COMSOL Multiphysics 5.4 software.

1. Introduction

Nowadays, optical devices based on surface plasmon polaritons (SPPs) are of interest to researchers in integrated circuit design [1]. SPPs are the surface electromagnetic waves that propagate along metal-dielectric interfaces and arise from the interaction between the electromagnetic waves and the free electrons of metals [1]. The ability to fabricate low-loss devices with dimensions of less than 100 nm and to confine the light beyond the diffraction limit led to designing all-optical SPP structures [2]. The basic idea for creating plasmonic devices is to control the destructive and constructive interferences between light signals in plasmonic waveguides [3–5]. In recent years, many passive and active SPP devices have been designed, such as switches [6, 7], logic gates [8–15], sensors [16–18], nanowires [19, 20], splitters [21], filters [22, 23], couplers [24], resonators [25], multiplexers, and demultiplexers [26–29]. There are two main types of plasmonic waveguides used in this way: MIM and IMI plasmonic waveguides. In IMI waveguides, the propagation length is longer, the propagation loss is lower, and it has a more straightforward fabrication process [8].

Other important applications and research studies are mentioned in this section. A numerical investigation of an all-optical SR flip-flop using plasmonic metal-insulator-metal (MIM) waveguides at the wavelength of 1,550 nm has been discussed in reference [30]. This research attempts to understand the behavior and performance of this device in optical signal processing applications. The study focuses on how the device operates and how the plasmonic properties can be utilized to achieve high-speed and low-power operation. The creation of an all-optical signal router utilizing plasmonic waveguides is covered in reference [31]. The main objective of this study is to suggest an effective and small architecture for an optical signal router that can control and route optical signals in communication networks. The authors aim to achieve improved performance, such as low-signal loss, high-speed operation, and smaller device footprint, by exploiting the special characteristics of plasmonic waveguides.

As for the most important previous works on the multiplexer, a 2×1 all-optical multiplexer with a threshold limit of 0.5 using a Kerr nonlinear nanoplasmonic switch, was used as discussed in reference [28]. This structure operates at 685 nm and 793.2 nm wavelengths. However, the size of this structure is relatively large, equal to $3000\,\text{nm} \times 2400\,\text{nm}$, and its fabrication will be complex. Furthermore, the optimal transmission efficiency of this Mux is 70%. A broadband mode converter and multiplexer based on dielectric-loaded plasmonic waveguides were discovered in reference [29]. This structure operates at a 1,550 nm wavelength, and the maximum transmission at this wavelength is low. In addition, this structure is relatively large and its construction will be complicated.

The plasmonic multiplexer based on nanogroove arrays with two operational wavelengths was designed in reference [32]. This structure operates at 650 nm and 850 nm wavelengths. However, the size of this structure is relatively large, which is equal to $7.5\,\mu\text{m} \times 6\,\mu\text{m}$, and its fabrication will be complex. In addition, the transmission threshold between logic 0 and logic 1 is less than 0.5. An all-optical 2×1 multiplexer using an MIM-based plasmonic waveguide has been proposed in reference [33]. This structure has a transmission threshold of 0.5 between the logic 0 and logic 1. However, its size is relatively large at $9.2\,\mu\text{m} \times 7.8\,\mu\text{m}$, and its production will be harrowing due to the complexity of its design.

This study proposes a structure of three straight waveguides coupled to two elliptical IMI-plasmonic waveguides to realize a 2×1 multiplexer with a high-transmission ratio. The designed structure has a minimum size of $400\,\text{nm} \times 400\,\text{nm}$, and the operating wavelength is 1,550 nm. The numerical results are obtained by FEM using COMSOL Multiphysics 5.4 software. The proposed plasmonic multiplexer can be used in the construction of an all-optical arithmetic logic unit (ALU) and all-optical signal processing nanocircuits. Section 2 describes the resonator selection, configuration, and parameters for the proposed design at 1,550 nm wavelength. Section 3 presents the proposed structure arrangement and theoretical idea of operation. The efficiency of the suggested structure and simulation results are detailed in Section 4. In Section 5, a comparison between the proposed designed structure and previous investigations is provided. In the last section, the main findings of the study are described.

2. Resonator, Structural Type, and Suggested Design Parameter Selection for 1,550 nm Wavelength

As a starting point for our study, the first structure was created, as shown in Figure 1(a), to build the Mux and to obtain the highest transmission at a wavelength of 1,550 nm. Two strips and a nanosquare resonator make up this suggestion, and the transmission result for this case is shown in Figure 2. Figures 1(b) and 2 illustrate what happened when we changed the geometry of the resonator from a nanosquare to a nanodisc. As depicted in Figure 1(c), we replaced the nanodisc resonator with a nanoring resonator, improving the transmission performance. Finally, the maximum transmission was achieved at 1,550 nm after replacing the resonator with a nanoelliptical resonator, as shown in Figures 1(d) and 2. Therefore, the nanoelliptical resonator is the optimal selection for the given structure. Moreover, the dimensions of the four structures in Figure 1 are detailed in Table 1.

In addition to the need for more than three ports to design Mux, a resonator and a stripe are added as shown in Figure 3. Choosing the type of multilayer (IMI or MIM) plasmonic waveguides, as shown in Figures 3(a) and 3(b), is also one of the most important design considerations. As previously mentioned, there are two common types of plasmonic waveguides which are the insulator-metal-insulator (IMI) waveguide as depicted in Figure 3(a) and the metal-insulator-metal (MIM) waveguide as depicted in Figure 3(b). The differences between these two waveguides are summarized in Table 2 [5, 8, 34, 35]:

As mentioned in Table 2, for low propagation losses and other advantages and as depicted in Figure 4, the best possible plasmonic waveguide for the proposed design is IMI, with maximum transmission occurring at 1,550 nm wavelength.

The transmission spectrum of the proposed structure is minimized or shifted depending on the structural size, shape, parameters, material's refractive index, port position, and incident field polarization and phase. In this section, structural parameters are used in validation. The major and minor ellipse axes, a and b, waveguides width, w, the distances between the elliptical waveguides and the stripes, d, and the length of the middle strip, L_{ms}, are considered as structural parameters in validation.

The effect of changing the minor ellipse axis, b, on the transmission coefficient is shown in Figure 5. The transmission spectra are obtained by considering S (port 2) and B (port 5) ports are ON and A port (port 1) is OFF.

For the largest and smallest minor axis values, three following cases are assumed: (1) 35 nm and 15 nm, (2) 40 nm and 20 nm, and (3) 45 nm and 25 nm. When the width of the waveguide is 20 nm, the largest and the smallest major axes are 80 nm and 60 nm, respectively. Moreover, the middle

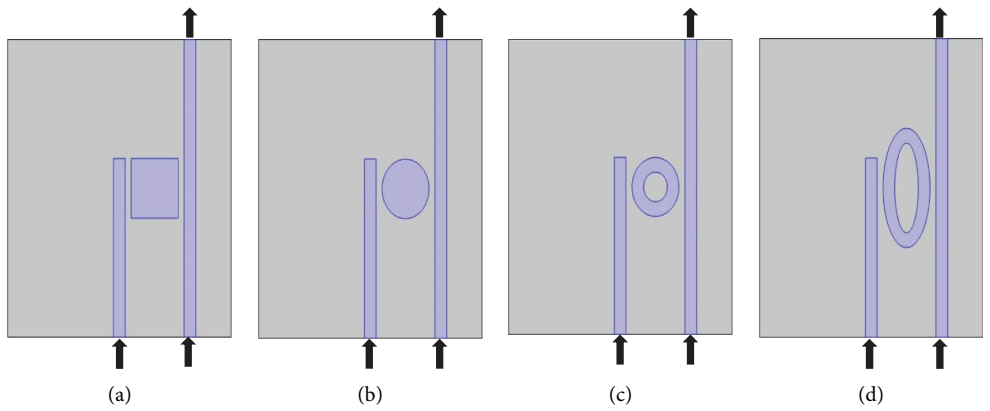

Figure 1: Initial structure comprised of a (a) nanosquare resonator, (b) nanodisc resonator, (c) nanoring resonator, and (d) nanoelliptical resonator.

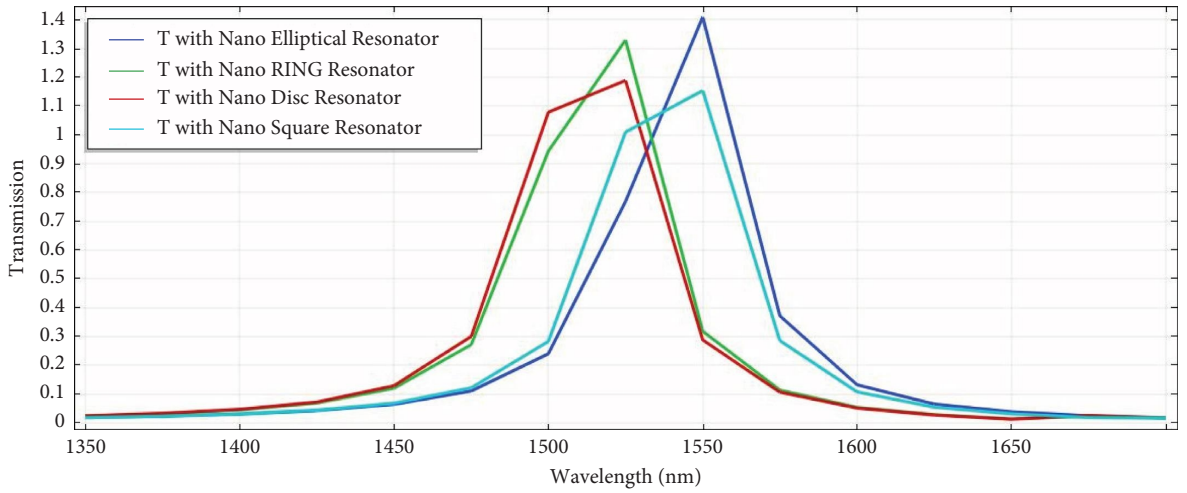

Figure 2: The transmission spectrum at the various resonator shapes.

Table 1: Parameters of the four structures with different resonators.

Parameter with description	Value (nm)
Height and width of all structures	400
Length of middle strips	240
Length and width of the nanosquare resonator	80
Largest and smallest major axis of nanoelliptical resonator	80, 60
Largest and smallest minor axis of nanoelliptical resonator	40, 20
Radius of nanodisc resonator	40
Largest and smallest radius of nanoring resonator	40, 20
Width of stripes	20
Distance between stripes and all resonators	10

stripe length and the distances between the elliptical waveguides and stripes are 240 nm and 10 nm, respectively. As shown in Figure 5, the resonance wavelength has a red shift by increasing the largest and smallest values of the minor axis, b; according to the results, when the largest minor axis is 40 nm, and the smallest minor axis value is assumed to be 20 nm, the resonance occurs in the desired wavelength. Therefore, we choose 40 and 20 nm as the largest and smallest values of the minor axis.

The result of changing the major axis on the transmission spectrum is shown in Figures 6(a) and 6(b). Assuming all other parameters remain unchanged, where the waveguide width is 20 nm, and the largest and the smallest minor axes are 40 nm and 20 nm, respectively. It is also assumed that the middle stripe length and the distances between the elliptical waveguides and the stripes are 240 nm and 10 nm, respectively.

In addition, in case the S port and the input ports are OFF, the transmission is shown in Figure 6(a) by considering three cases for the largest and smallest major axis, a, as follows: (1) 75 nm and 55 nm, (2) 80 nm and 60 nm, and (3) 85 nm and 65 nm. Figure 6(b) shows the transmission of the structure with three values for the largest and smallest major axes, a, in the case of S port and B port are ON, and the A port is OFF.

To achieve the desired result in operational wavelength and to obtain the best contrast ratio, we chose 80 nm for the largest major axis "a" of the ellipse and 60 nm for the smallest.

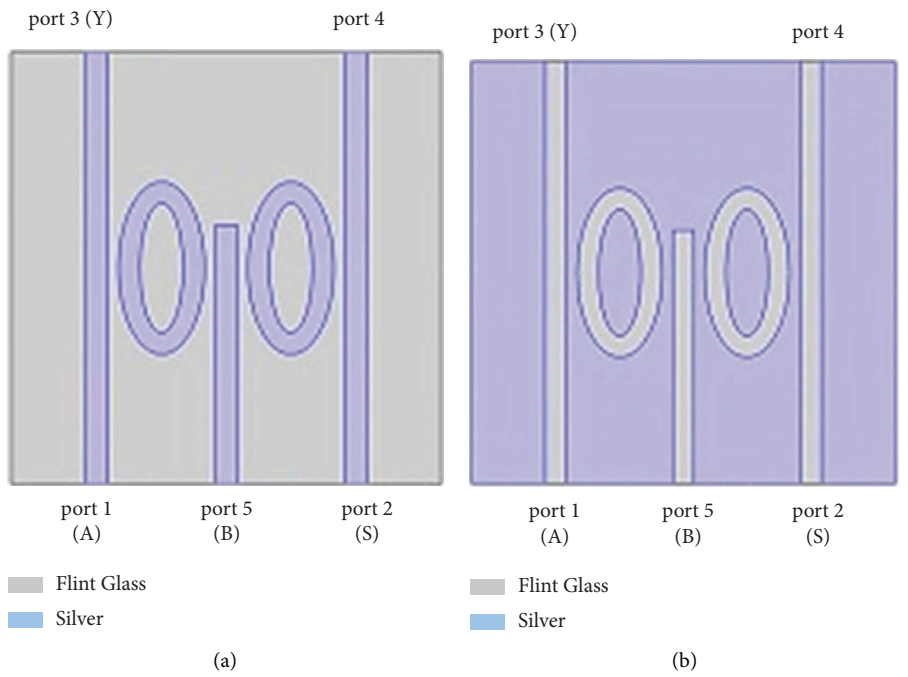

Figure 3: The proposed design with (a) IMI and (b) MIM plasmonic waveguides.

Table 2: A comparison between IMI and MIM waveguides.

	IMI waveguides	MIM waveguides
Layer configuration	Dielectric-metal-dielectric	Metal-dielectric-metal
Field confinement	Less	More
Propagation length	More	Less
Propagation loss	Low	Moderate to high
Dispersion	Can be engineered	Less control
Integration	On-chip integration	Limited integration options
Fabrication	Easy	Not easy

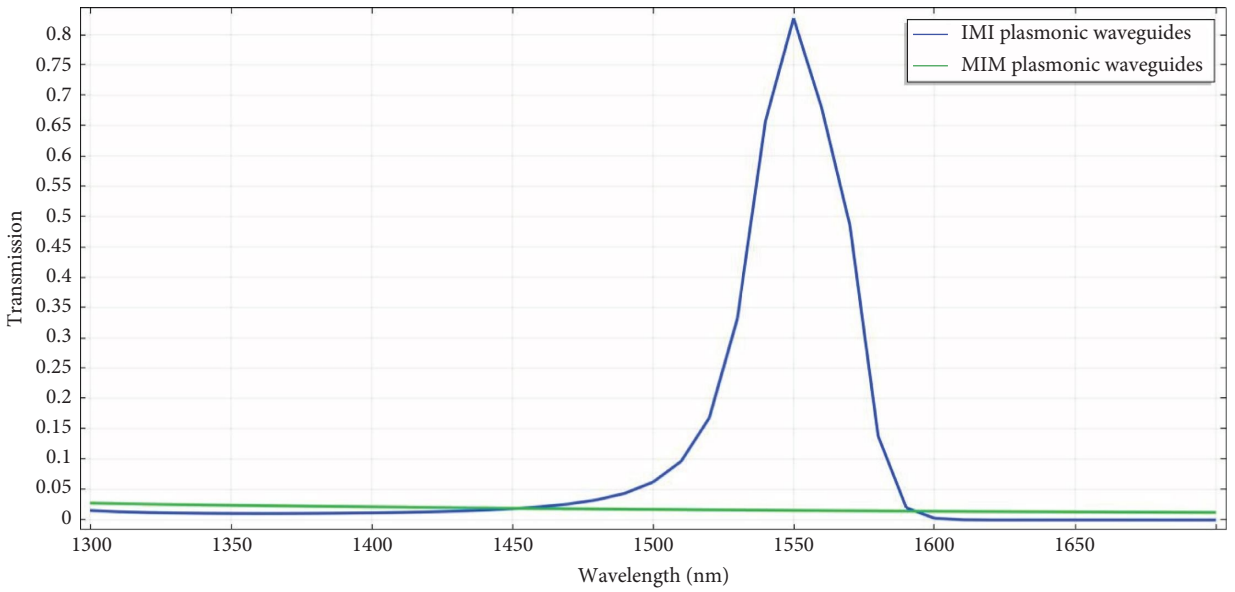

Figure 4: The transmission spectrum at IMI and MIM plasmonic waveguides.

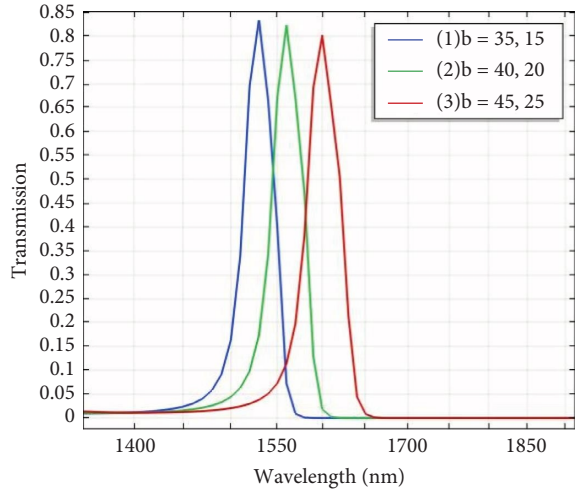

Figure 5: The transmission spectra of the proposed plasmonic Mux at different states of the largest minor axis "*b*" of the ellipse and the smallest, when S and B ports are ON and A port is OFF.

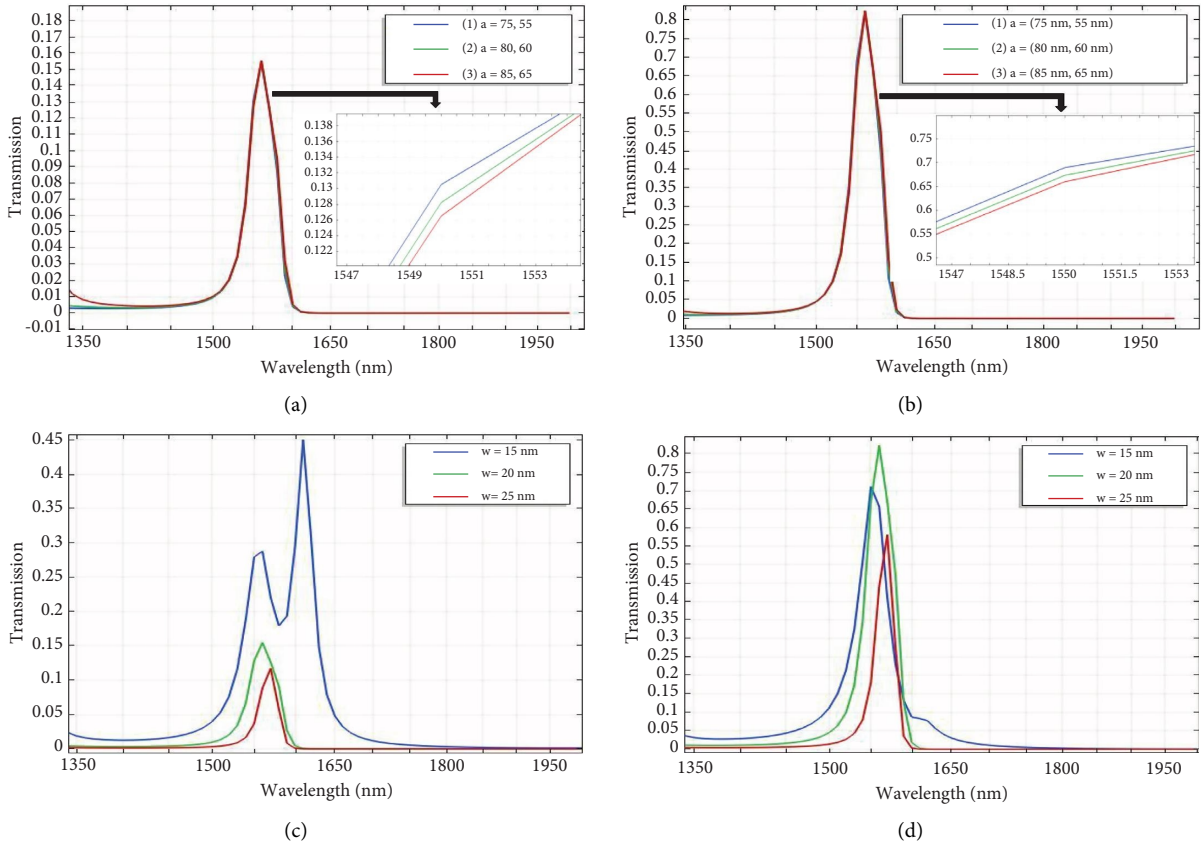

Figure 6: Continued.

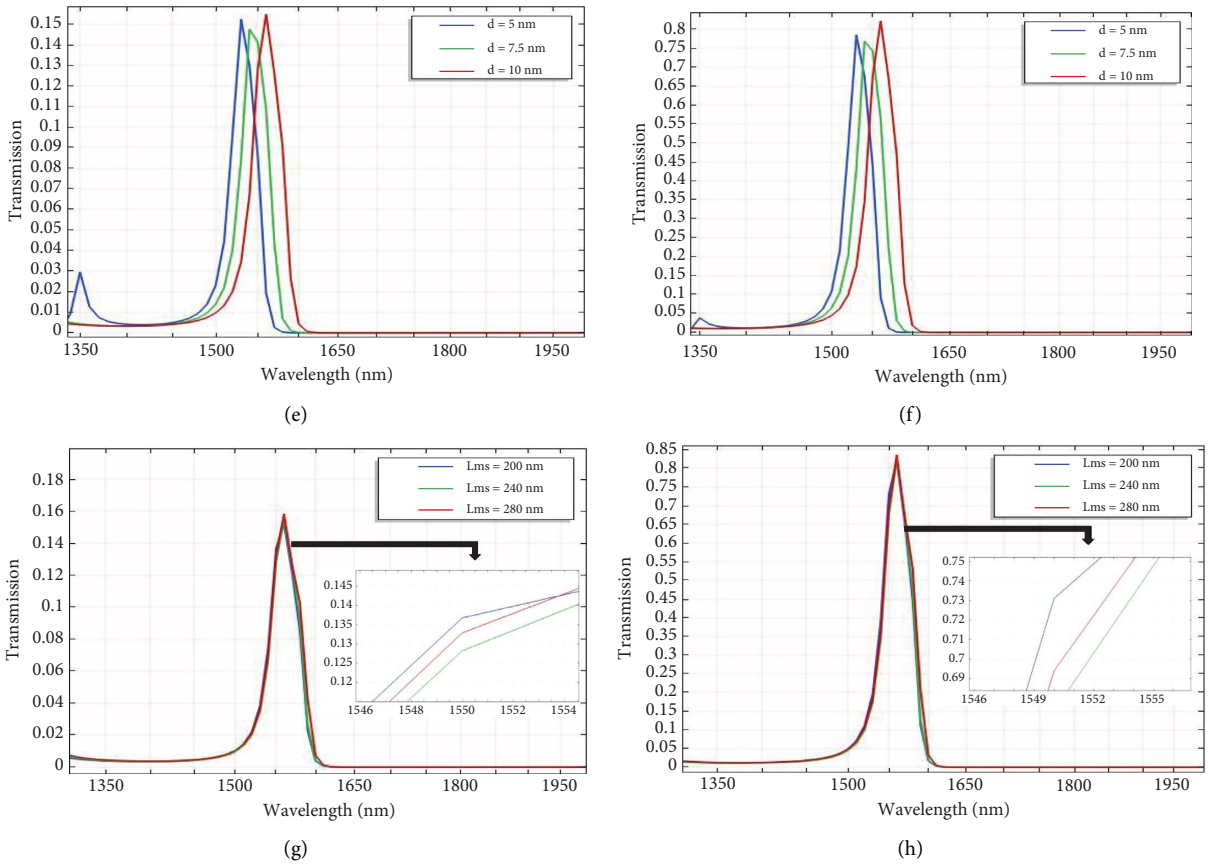

FIGURE 6: The transmission spectra of the proposed plasmonic Mux when the power is the maximum output optical power in case of OFF state and when the minimum output optical power in case of ON state, respectively, at different states of: (a), (b) largest and smallest major axess "a" of the ellipse. (c), (d) Stripes width "w". (e), (f) Distances between the elliptical waveguides and stripes "d". (g), (h) Middle stripe length "L_{ms}".

By choosing the desired ellipse's structural parameters and the distances between the elliptical waveguides and stripes of 10 nm and middle stripe length of 240 nm, the transmission spectrum for three values of w, 15 nm, 20 nm, and 25 nm, is illustrated in Figures 6(c) and 6(d). In Figure 6(c), the case of the S port and input ports are OFF. Figure 6(d) shows the transmission of the S port when the B port is ON and A port is OFF. The width of the waveguide is considered to be 20 nm to obtain the best contrast ratio.

The transmission spectrum for three values of the distance between the elliptical waveguides and the stripes, 5, 7.5, and 10 nm, with proper structural dimensions and middle stripe length, is shown in Figures 6(e) and 6(f). The transmission spectrum shown in Figure 6(e) relates to the S port and input ports being OFF. Figure 6(f) shows the transmission when the S port and B port are ON and the A port is OFF; according to the results for getting the best contrast ratio in Figures 6(e) and 6(f), we chose 10 nm for the distance between the elliptical waveguide and the stripes. Finally, by assuming the obtained structural parameters, the effect of changing the middle stripe length on the transmission spectrum is illustrated in Figures 6(g) and 6(h). Figure 6(g) shows the transmission when the S and input ports are OFF. In addition, the transmission spectrum in the case of the S port and B port is ON, and the A port is OFF, as shown in Figure 6(h). According to the results, the middle stripe length is chosen as 240 nm to achieve the best contrast ratio. All of the cases studied mentioned in Figure 6 are listed in Table 3.

3. Structure Layout

Based on the previous sections and the shape and dimensions selected, the proposed 2 × 1 Mux based on IMI-plasmonic waveguide consisting of two elliptical waveguides and three straight stripes, as shown in Figures 7(a) and 7(b), has been proposed. The metal region is silver, and the insulator medium is realized by flint glass (pure), and the substrate is made of a semiconductor material such as silicon in the case of the used three-dimensional (3D) structure. The permittivity of silver is characterized by the findings of Johnson and Christy [36], and the refractive index of the flint glass is 1.61 [37]. The design area of the proposed architecture is 400 nm × 400 nm. Moreover, the lengths of the two side stripes are 400 nm, and Table 4 details the length of the middle stripe L_{ms} and all dimensions of the proposed structure. The operating wavelength is 1,550 nm, the best choice for optical communication applications.

Table 3: Validation of the structure shown in Figure 6.

Dimensions	Dimension length (nm)	(P_{out} |OFF)	(P_{out} |ON)	Contrast ratio	Best dimension (nm)
Largest, smallest major axis "a"	75, 55	0.13	0.69	7.24	80, 60
	80, 60	0.127	0.675	7.25	
	85, 65	0.125	0.66	7.22	
Stripes width "w"	15	0.28	0.71	4.04	20
	20	0.127	0.675	7.25	
	25	0.037	0.18	Fault	
Distances between the elliptical waveguides and stripes "d"	5	0.09	0.44	Fault	10
	7.5	0.142	0.741	7.17	
	10	0.127	0.675	7.25	
Middle stripe "L_{ms}"	200	0.138	0.73	7.23	240
	240	0.127	0.675	7.25	
	280	0.133	0.695	7.1	

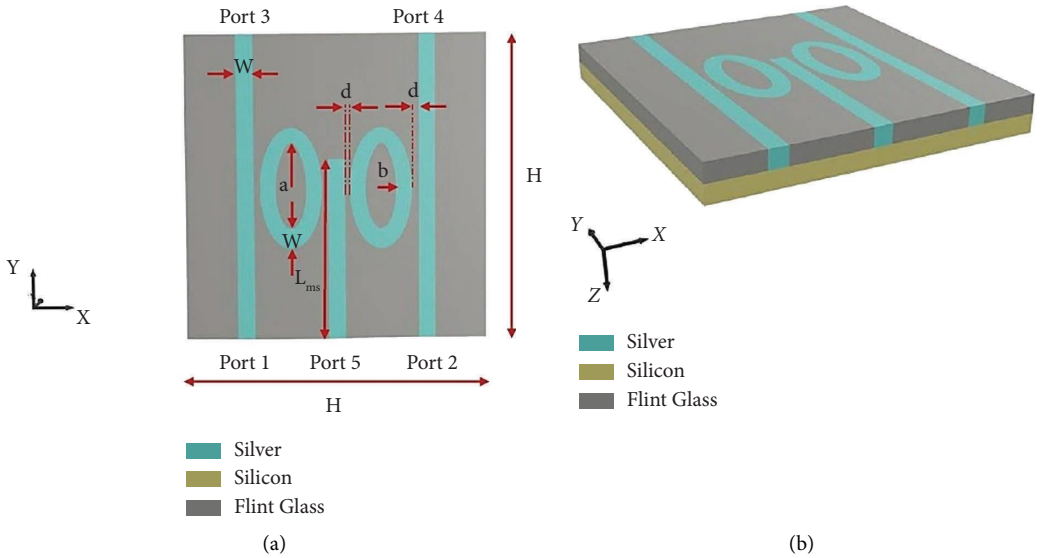

Figure 7: (a) 2D and (b) 3D of the proposed plasmonic 2 × 1 Mux with 400 nm × 400 nm area.

Table 4: Parameters of the proposed structure.

Parameter	Description	Value (nm)
H	Height and width of the structure	400
L_{ms}	Length of middle stripe	240
a	Largest and smallest major axis "a"	80, 60
b	Largest and smallest minor axis "b"	40, 20
W	Width of stripes and nanoellipse resonator	20
d	Distance between stripes and nanoellipse resonator	10

The two-dimensional (2D) FEM technique is used to solve the Maxwell equations numerically, and a convolutional perfectly matched layer (CPML) is considered to absorb the boundary condition of the simulation domain. A transverse magnetic (TM)-polarized plane wave with Ex, Ey, and Hz, electromagnetic field components, excites the structure. The designed Mux has five ports as follows: ports 1 and 5 are input ports, port 2 is considered as selector port, port 3 is the output port, and port 4 is always ON. The other details of the input source parameters in the software used are given in Table 5.

The proposed Mux is based on constructive and destructive interferences between input signals and the selector signal. The destructive and constructive interferences between the input light signals and the selector light signal depend on the phase of the incident light signal as well as the location of the input ports and selector ports. When the incident signals at the input ports and the selector port have the same phase and direction of propagation, constructive interference occurs. When the phase degree or direction of the incident signal's propagation at the input ports and selector ports are different, destructive interference occurs.

Table 5: The details of the input source parameters.

Input source parameters	Description or values
Input power	1 μw
Software	COMSOL multiphysics
Mesh size	Extremely fine
Type of physics	Electromagnetic wave frequency domain
Type of study	Parametric sweep (1200 nm–2000 nm)
Type of existing mode	TM (Ex, Ey, Hz)
Type of materials	Flint glass, silver

According to (1), the phase difference produces destructive interference between the signals [38, 39].

$$m = \frac{(4n_{\text{eff}} d \cos\ \theta)}{\lambda}, \tag{1}$$

where, m, n_{eff}, d, θ, and λ are the interference order as an integer larger than zero, an effective refractive index of the silver material, the thickness of the metal material, the phase of the incident signal, and the incident wavelength, respectively.

The sign of (1) is positive by assuming $\theta = 0^{\circ}$, which means that the propagation direction of a signal is identical to its mode. Therefore, constructive interference occurs with the other modes with the same phase, and the transmission will increase. In addition, when θ is 90 degrees, the result of (1) will be zero. Therefore, no interference will occur for this mode (no constructive interference, no destructive interference), and transmission will either increase or decrease depending on the other input and selector phases as well as the other parameters. Moreover, when θ is 180 degrees, the result of (1) will be negative; thus, the direction of the mode is the opposite of the signal's propagation. Therefore, destructive interference arises between modes with distinct phase differences, and for that, the transmission will be increased.

The performance of the plasmonic Mux is described by three parameters: transmission (T), contrast ratio (CR), modulation depth (MD), insertion loss (IL), and contrast loss (CL).

Transmission is linked to the transmitted optical power from the input ports, port 1 and port 5, and the selector port, port 2, to the output port, port 3. The transmission is defined as follows [8]:

$$T = \frac{P_{\text{out}}}{P_{in}}, \tag{2}$$

where T is the transmission, P_{in} can be considered as the input power at ports 1, 2, 4, and 5. P_{out} is the output optical power at port 3. The transmission can be achieved by selecting the transmission threshold between ON, logic 1, and off, logic 0, states. For the designed 2×1 Mux, the transmission threshold value between logic 1 and logic 0 at the output is 0.5.

The contrast ratio is related to the minimum output optical power in the ON state ($P_{\text{out}}|ON$) and the maximum output optical power in the OFF state ($P_{\text{out}}|OFF$) and is obtained by the following [40]:

$$\text{CR (dB)} = 10 \log\left(\frac{P\text{out} \mid \text{ON}}{P\text{out} \mid \text{OFF}}\right). \tag{3}$$

A higher CR indicates that the designed structure is functioning as expected. The description of the value of CR is given in Reference [41]. Modulation depth (MD) is the third parameter; it indicates the relationship between the maximum transmission during the ON state (TON|Max) and the minimum transmission during the OFF state (TOFF|Min). The following equation is its definition [42]:

$$\text{MD} = \left(\frac{T_{\text{ON}}|\text{Max} - T_{\text{OFF}}|\ \text{Min}}{T_{\text{ON}} \mid\ \text{Max}}\right). \tag{4}$$

MD evaluates whether the dimensions selected for the proposed design are optimal or not. According to authors in reference [42], MD's values are determined.

Insertion loss (IL) is the fourth criterion, which is related to the minimum optical output power that occurs in the ON state and the input optical power. It is determined using the following equation [43]:

$$\text{Insertion loss (dB)} = -10 \log\left(\frac{P\text{out}_{\text{ON}} \mid\ \text{Min}}{P\text{in}}\right). \tag{5}$$

This parameter measures the losses incurred when one device is inserted into another. The value definitions are provided in Table 6.

The last parameter extracted is contrast loss (CL), which measures the losses due to the contrast ratio; when the contrast ratio is elevated and insertion loss is low, the induced losses are low, and vice versa; this means that the total loss is low whenever the CL is high, according to the following equation:

$$\text{Contrast Loss (dB)} = \text{CR (dB)}–\text{IL (dB)}. \tag{6}$$

Table 7 describes each possible value for this parameter.

4. Simulation Results

The proposed structure has been illuminated by a plane wave with a wavelength from 1,200 to 2,000 nm to study the MUX operation, as shown in Figure 7.

Block diagram, truth, and condensed tables of a 2×1 Mux are presented in Figures 8(a)–8(c), respectively. In the designed Mux, port 4 is always ON and input ports are considered as A and B states. Selector and output ports are assumed as S and Y states, respectively.

As shown in Figure 9(a), when the states of input ports, A and B states, are OFF or only B state is ON with 180° phase and the selector port, S, is OFF, the state of the output port of the multiplexer, Y, is OFF. According to the results, when the input ports are OFF, the transmission value is 0.12 at the operating wavelength. If only B is ON, the transmission value is 0.08 at a wavelength of 1,550 nm. The obtained transmission values at the operational wavelength are below the transmission threshold. As illustrated in Figure 9(a), when A and B are ON, or only A is ON, and S is OFF, constructive interference occurs between port A and port 4 or between port A and port B and the transmission increases.

Table 6: Description of the insertion loss values.

IL (dB) ranges	Description	Assessment of IL
More than 5	Very high	Bad and inefficient
More than 3–5	High	Accepted
More than 1–3	Medium	Moderate
More than 0-1	Low	Good
More than −1–0	Very low	Very good and efficient
−1 and less	Ultralow	Excellent and efficient

Table 7: Explanation of the values of the contrast loss.

CL (dB) ranges	Description	Assessment of CL
Negative value	Ultralow	Bad and inefficient
Less than or equal 4	Very low	Accepted
More than 4 to 8	Low	Moderate
More than 8 to 12	Medium	Good
More than 12 to 16	High	Very good and efficient
More than 16 to 20	Very high	Excellent and efficient
More than 20 dB	Ultrahigh	Excellent and optimum

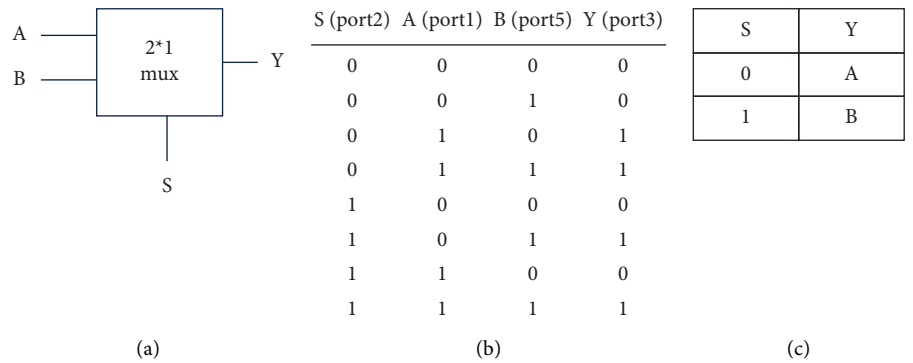

Figure 8: Multiplexer (a) conventional symbol, (b) truth table, and (c) condensed truth table.

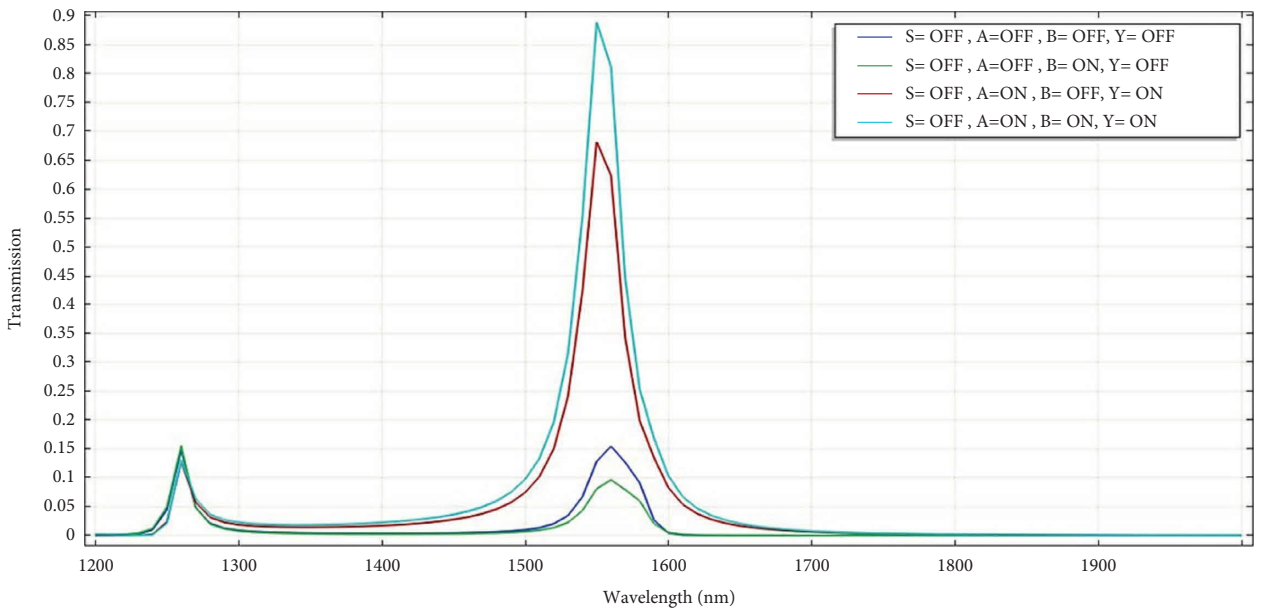

(a)

Figure 9: Continued.

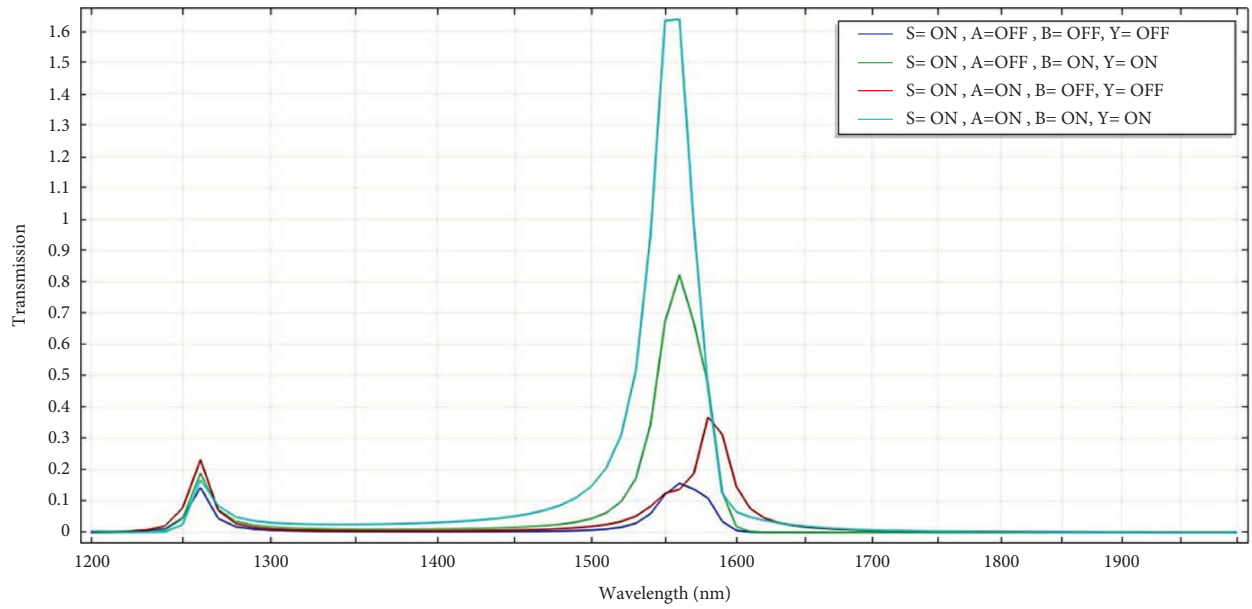

(b)

Figure 9: The transmission spectra of the proposed plasmonic Mux at different states when (a) selector port is OFF and (b) selector port is ON.

Table 8: Summarized simulation results in Figures 3(a) and 3(b).

S (port 2)	A (port 1)	B (port 5)	T threshold	T	Y (port3)	CR (dB)	MD (%)	IL (dB)	CL (dB)
OFF	OFF	OFF	0.5	0.12	OFF	7.25	95.09	1.67	5.57
OFF	OFF	ON		0.08	OFF				
OFF	ON	OFF		0.68	ON				
OFF	ON	ON		0.89	ON				
ON	OFF	OFF		0.12	OFF				
ON	OFF	ON		0.68	ON				
ON	ON	OFF		0.12	OFF				
ON	ON	ON		1.63	ON				

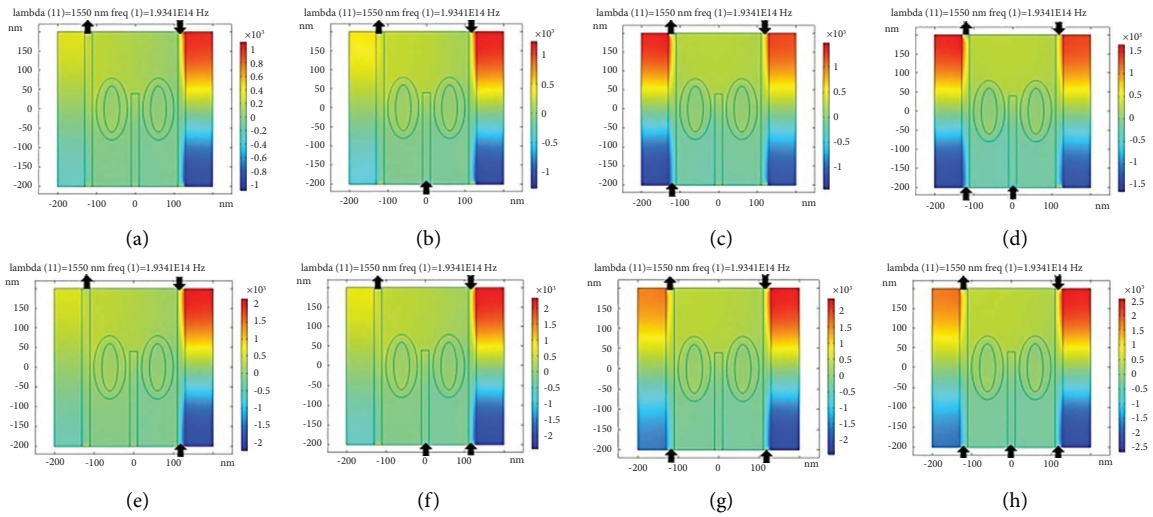

Figure 10: The magnetic field distribution (Hz-component) for all cases due to its truth table (a) S = OFF and input ports = OFF, (b) S = OFF, A = OFF, and B = ON, (c) S = OFF, A = ON, and B = OFF, (d) S = OFF and input ports are ON. (e) S = ON and input ports = OFF, (f) S = ON, A = OFF, and B = ON, (g) S = ON, A = ON, and B = OFF, and (h) S = ON and input ports are ON.

Table 9: Comparison between the proposed structure and the previous works.

Reference	Topology	Size	Metal model	Number of resonators	Threshold limit	Operating wavelength	Performance measured by	Max. T	Structure complexity	Method used
[28]	Nanoracetrack resonator side coupled to air (MIM) waveguide	3000 nm × 2400 nm	Drude model	One	0.5	685 nm, 793.2 nm	Two parameters	70%	More	FDTD
[29]	Dielectric-loaded plasmonic waveguides	5.7 μm × 2.105 μm and more than 8 μm × 1 μm	Not available	Two	Less than 0.5	1550 nm	One parameter	80%	More	FDTD
[32]	Plasmonic unidirectional coupler (MIM) waveguide	7.5 μm × 6 μm	Drude model	Did not use resonator	0.33	650 nm, 850 nm	Two parameters	100%	More	FDTD
[33]	(MIM) plasmonic waveguide	9.2 μm × 7.8 μm	Not available	Y shape wave guide	0.5	1550 nm	Two parameters	Less than 10%	More	FDTD
[44]	MIM plasmonic slot cavities	1.055 μm × 1.055 μm	Drude model	Four	0.5	650 nm, 850 nm	Four parameters	About 100%	More	FEM
[45]	Surface plasmonic resonance in optical ring resonators MIM configuration	About 2.5 μm × 1 μm	Drude model	Three	About 0.45	1133 nm, 1219 nm and 1456 nm	Three parameters	About 100%	More	FDTD
[46]	Hybrid plasmonic waveguides	About 41 μm × 20 μm	Not available	Did not use resonator	Not available	1550 nm	One parameter	99.2%	More	FEM
This work	Nanoellipse IMI nanoplasmonic waveguides	400 nm × 400 nm	Johnson and christy data	one	0.5	1550 nm	Five parameters	163%	Lesser	FEM

For ON output states, the transmission values are 0.68 and 0.89, above the transmission threshold.

As shown in Figure 9(b), when the A and B states are OFF and S state is ON, with a phase of 180°, the destructive interference will occur between port 4 and selector port (S). In this case, transmission is 0.12, and the Y state is OFF. When the states of A and S are ON, and the phase of A signal equals 180°, the destructive interference will occur between port A and selector port (S), and the transmission value is 0.12, so the state of output port (Y) will be OFF. According to Figure 9(b) and the truth table in Figure 8(b), when the selector and input B ports are ON and port A is OFF, the constructive interference occurs between B port and selector port, and the output port is ON. In this case, the transmission value is 0.68. When inputs and selector ports are ON, the transmission exceeds 100% (1.63), resulting from constructive interference between the inputs and selector signals. The contrast ratio of this structure is 7.25 dB, and its performance is moderate, according to the authors in reference [41]. In addition, the recommended structure dimensions are excellent and optimal based on the MD value of 95.09%. Moreover, according to Tables 6 and 7, the IL and CL are moderate. The simulation results are summarized in Table 8.

The z-component of the magnetic field, Hz, distribution, for all cases due to its truth table is shown in Figures 10(a)–10(h). The color bar in Figures 10(a)–10(h) illustrates the variation in light power intensity; the evolution from blue to red demonstrates that the light power intensity increases from low to high.

5. Comparison of the Proposed Work with Prior Works

The proposed structure is compared with the previous works as summarized in Table 9. As can be seen from Table 9, the proposed structure has good characteristics and the overall performance of our proposed work is more reasonable than the others.

6. Conclusion

An all-optical 2 × 1 (Mux) with a new configuration based on elliptical IMI-plasmonic waveguides has been presented in this paper. The proposed structure, which operates at a wavelength of 1,550 nm, has a compact size (400 nm × 400 nm), is simple, and has low loss. The function of the structure is based on constructive and destructive interferences between input signal(s) and the selector signal. The performance of the proposed plasmonic Mux is characterized by five parameters as follows: transmission (T), contrast ratio (CR), modulation depth (MD), insertion loss (IL), and contrast loss (CL) at 1,550 nm. The transmission threshold between logic 0 and logic 1 states was considered to be 0.5. According to the results, the maximum transmission efficiency of the device was 163%, and the recommended structure dimensions are excellent and optimal based on the MD value of 95.09%. The simulation results were obtained using the finite element method (FEM) with COMSOL Multiphysics 5.4 software.

Data Availability

The data generated during the current study will be made available by the corresponding author upon reasonable request.

Conflicts of Interest

The authors declare that there are no conflicts of interest regarding the publication of this article.

Acknowledgments

We would like to express our deep appreciation for the article authored by Abdulnabi, Saif H., and Mohammed N. Abbas which was published in the AIP Conference Proceedings [47] in the field of research on optical demultiplexers and their nanoscale applications.

References

[1] S. I. Bozhevolnyi, *Plasmonic Nanoguides and Circuits*, Pan Stanford Publishing, Singapore, 2008.

[2] E. Ozbay, "Plasmonics: merging photonics and electronics at nanoscale dimensions," *Science*, vol. 311, no. 5758, pp. 189–193, 2006.

[3] Y. Fu, X. Hu, C. Lu, S. Yue, H. Yang, and Q. Gong, "All-optical logic gates based on nanoscale plasmonic slot waveguides," *Nano Letters*, vol. 12, no. 11, pp. 5784–5790, 2012.

[4] S. Yu, X. Piao, and N. Park, "Slow-light dispersion properties of multiatomic multiband coupled-resonator optical waveguides," *Physical Review A*, vol. 85, no. 2, Article ID 023823, 2012.

[5] S. H. Abdulnabi and M. N. Abbas, "Design an all-optical combinational logic circuits based on nano-ring insulator-metal-insulator plasmonic waveguides," *Photonics*, vol. 6, no. 1, p. 30, 2019.

[6] J. Tao, Q. J. Wang, and X. G. Huang, "All-optical plasmonic switches based on coupled nanodisk cavity structures containing nonlinear material," *Plasmonics*, vol. 6, no. 4, pp. 753–759, 2011.

[7] N. Nozhat and N. Granpayeh, "All-optical nonlinear plasmonic ring resonator switches," *Journal of Modern Optics*, vol. 61, no. 20, pp. 1690–1695, 2014.

[8] S. H. Abdulnabi and M. N. Abbas, "All-optical logic gates based on nanoring insulator–metal– insulator plasmonic waveguides at optical communications band," *Journal of Nanophotonics*, vol. 13, no. 1, pp. 016–009, 2019.

[9] N. Nozhat and N. Granpayeh, "All-optical logic gates based on nonlinear plasmonic ring resonators," *Applied Optics*, vol. 54, no. 26, pp. 7944–7948, 2015.

[10] D. Pan, H. Wei, and H. Xu, "Optical interferometric logic gates based on metal slot waveguide network realizing whole fundamental logic operations," *Optics Express*, vol. 21, no. 8, pp. 9556–9562, 2013.

[11] L. Wang, L. Yan, Y. Guo, K. Wen, W. Pan, and B. Luo, "Optical quasi logic gates based on polarization-dependent four-wave mixing in subwavelength metallic waveguides," *Optics Express*, vol. 21, no. 12, pp. 14442–14451, 2013.

[12] Y. Bian and Q. Gong, "Compact all-optical interferometric logic gates based on onedimensional metal-insulator-metal structures," *Optics Communications*, vol. 313, pp. 27–35, 2014.

[13] K. J. A. Ooi, H. S. Chu, P. Bai, and L. K. Ang, "Electro-optical graphene plasmonic logic gates," *Optics Letters*, vol. 39, no. 6, pp. 1629–1632, 2014.

[14] I. S. Maksymov, "Optical switching and logic gates with hybrid plasmonic-photonic crystal nanobeam cavities," *Physics Letters A*, vol. 375, no. 5, pp. 918–921, 2011.

[15] H. K. Al-Musawi, A. K. Al-Janabi, S. A. W. Al-abassi, N. A. H. A. Abusiba, and N. A. H. Q. Al-Fatlawi, "Plasmonic logic gates based on dielectric-metal-dielectric design with two optical communication bands," *Optik*, vol. 223, Article ID 165416, p. þ, 2020.

[16] M. R. Rakhshani, A. Tavousi, and M. A. Mansouri-Birjandi, "Design of a plasmonic sensor based on a square array of nanorods and two slot cavities with a high figure of merit forglucose concentration monitoring," *Applied Optics*, vol. 57, no. 27, pp. 7798–7804, 2018.

[17] S. Enoch, R. Quidant, and G. Badenes, "Optical sensing based on plasmon coupling in nanoparticle arrays," *Optics Express*, vol. 12, no. 15, pp. 3422–3427, 2004.

[18] D. Van Oosten, M. Spasenović, and L. Kuipers, "Nanohole chains for directional and localized surface plasmon excitation," *Nano Letters*, vol. 10, no. 1, pp. 286–290, 2010.

[19] C. Min, P. Wang, X. Jiao, Y. Deng, and H. Ming, "Beam focusing by metallic nano-slit array containing nonlinear material," *Applied Physics B*, vol. 90, no. 1, pp. 97–99, 2008.

[20] R. M. Dickson and L. A. Lyon, "Unidirectional plasmon propagation in metallic nanowires," *Journal of Physical Chemistry B*, vol. 104, no. 26, pp. 6095–6098, 2000.

[21] J. Chen, Z. Li, M. Lei, X. Fu, J. Xiao, and Q. Gong, "Plasmonic Y-splitters of high wavelength resolution based on strongly coupledresonator effects," *Plasmonics*, vol. 7, no. 3, pp. 441–445, 2012.

[22] H. Lu, X. Liu, Y. Gong, L. Wang, and D. Mao, "Multi-channel plasmonic waveguide filters with disk-shaped nanocavities," *Optics Communications*, vol. 284, no. 10-11, pp. 2613–2616, 2011.

[23] A. Setayesh, S. R. Mirnaziry, and M. S. Abrishamian, "Numerical investigation of tunable band-pass\band-stop plasmonic filters with hollow-core circular ring resonator," *Journal of the Optical Society of Korea*, vol. 15, no. 1, pp. 82–89, 2011.

[24] N. Nozhat and N. Granpayeh, "Switching power reduction in the ultracompact Kerr nonlinear plasmonic directional coupler," *Optics Communications*, vol. 285, no. 6, pp. 1555–1559, 2012.

[25] Y. Guo, L. Yan, W. Pan et al., "Transmission characteristics of the aperture-coupled rectangular resonators based on metal-insulator-metal waveguides," *Optics Communications*, vol. 300, pp. 277–281, 2013.

[26] G. Wang, H. Lu, X. Liu, D. Mao, and L. Duan, "Tunable multi-channel wavelength demultiplexer based on MIM plasmonic nanodisk resonators at telecommunication regime," *Optics Express*, vol. 19, no. 4, pp. 3513–3518, 2011.

[27] C. T. Wu, C. C. Huang, and Y. C. Lee, "Plasmonic wavelength demultiplexer with a ring resonator using high-order resonant modes," *Applied Optics*, vol. 56, no. 14, pp. 4039–4044, 2017.

[28] S. Bashiri and K. Fasihi, "A 2 × 1 all-optical multiplexer using Kerr nonlinear nano-plasmonic switch," *Optical and Quantum Electronics*, vol. 51, no. 11, p. 374, 2019.

[29] Y. Qiu, J. Tao, Z. Liu, and X. Li, "Broadband mode converter and multiplexer based on dielectric-loaded plasmonic waveguides," *Current Applied Physics*, vol. 20, no. 2, pp. 244–248, 2020.

[30] L. Singh, N. Agrawal, K. K. Gola, C. Saha, and P. Pareek, "Numerical investigation of all optical SR flip-flop using plasmonic metal–insulator-metal (MIM) waveguides," *Optical and Quantum Electronics*, vol. 54, no. 6, p. 381, 2022.

[31] L. Singh, A. Iadicicco, N. Agrawal, C. Saha, and R. Chauhan, "A compact formulation of all optical signal router by using plasmonic waveguides," *Optical and Quantum Electronics*, vol. 54, no. 8, p. 478, 2022.

[32] A. Udupi and S. K. Madhava, "Plasmonic coupler and multiplexer/demultiplexer based on nano-groove-arrays," *Plasmonics*, vol. 16, no. 5, pp. 1685–1692, 2021.

[33] I. Charles, "An all optical 2×1 multiplexer using a metal-insulator-metal based plasmonic waveguide for processing at a rapid pace," *Photonics*, vol. 10, no. 1, 2023.

[34] R. F. Oulton, V. J. Sorger, T. Zentgraf et al., "Plasmon lasers at deep subwavelength scale," *Nature*, vol. 461, no. 7264, pp. 629–632, 2009.

[35] G. Sun, H. Long, Q. Gong, and S. Wang, "Integrated optical plasmonic devices for subwavelength confinement and nanoscale light manipulation," *Advances in Optics and Photonics*, vol. 7, no. 3, pp. 684–712, 2015.

[36] P. B. Johnson and R. W. Christy, "Optical constants of the noble metals," *Physical Review B*, vol. 6, no. 12, pp. 4370–4379, 1972.

[37] C. R. Kurkjian and W. R. Prindle, "Perspectives on the history of glass composition," *Journal of the American Ceramic Society*, vol. 81, no. 4, pp. 795–813, 2005.

[38] W. Chen, R. L. Nelson, and Q. Zhan, "Geometrical phase and surface plasmon focusing with azimuthal polarization," *Optics Letters*, vol. 37, no. 4, pp. 581–583, 2012.

[39] D. Choi, C. K. Shin, D. Yoon, D. S. Chung, Y. W. Jin, and L. P. Lee, "Plasmonic optical interference," *Nano Letters*, vol. 14, no. 6, pp. 3374–3381, 2014.

[40] A. Dolatabady and N. Granpayeh, "All-optical logic gates in plasmonic metal-insulator–metal nanowaveguide with slot cavity resonator," *Journal of Nanophotonics*, vol. 11, no. 2, pp. 026001–001, 2017.

[41] M. N. Abbas and S. H. Abdulnabi, "Plasmonic reversible logic gates," *Journal of Nanophotonics*, vol. 14, no. 01, pp. 1–003, 2020.

[42] S. H. Abdulnabi and M. N. Abbas, "Design and simulation of an all-optical 2 × 1 plasmonic multiplexer," *Journal of Nanophotonics*, vol. 16, no. 01, Article ID 016009, 2022.

[43] K. Choudhary, S. Mishra, S. Singh, and S. Kumar, "Design of all-optical OR/NAND logic gate using plasmonic metal-insulator-metal waveguide," *Physics and Simulation of Optoelectronic Devices XXIX*, vol. 11680, 2021.

[44] U. Aparna and M. S. Kumar, "Ultra-compact plasmonic unidirectional wavelength multiplexer/demultiplexer based on slot cavities," *Optical Review*, vol. 29, no. 1, pp. 51–58, 2022.

[45] M. Mansuri, A. Mir, and A. Farmani, "A tunable nonlinear plasmonic multiplexer/demultiplexer device based on nanoscale ring resonators," *Photonic Network Communications*, vol. 42, no. 3, pp. 209–218, 2021.

[46] M. Yin, Q. Deng, Y. Li, X. Wang, and H. Li, "Compact and broadband mode multiplexer and demultiplexer based on asymmetric plasmonic–dielectric coupling," *Applied Optics*, vol. 53, no. 27, pp. 6175–6180, 2014.

[47] S. H. Abdulnabi and M. N. Abbas, "Theoretical investigation of a nano scale all-optical 1× 2 demultiplexer," *AIP Conference Proceedings*, vol. 2651, no. 1, 2023.